

DERIVATION OF STOCHASTIC BIASED AND CORRELATED RANDOM WALK MODELS

ELIFE DOGAN-CIFTCI AND UMMUGUL BULUT

Department of Education, North American University, 11929 W Airport Blvd,
Stafford, TX 77477 USA

Department of Mathematics, Texas A&M University-San Antonio, One University
Way, San Antonio, TX 78224 USA

ABSTRACT. In biased and correlated random walk (BCRW) models, the movement is characterized by correlated successive step orientations along with a bias in the globally preferred direction. In this study, stochastic partial differential equations (SPDEs) for BCRW are derived for one, two, and three dimensions. First, discrete-time stochastic models are developed by determining the changes for a small time interval. As the time interval approaches zero, systems of Itô stochastic differential equations are found. Then, SPDEs are derived as the space interval approaches zero. Finally, numerical solutions of the stochastic equations are compared with the independently formulated Monte Carlo calculations.

Key Words Biased and correlated random walk, biased telegraph equations, stochastic differential equations, stochastic partial differential equations, Itô System.

Subject Classification: 82C70; 60H15; 82C41; 60H10; 65C30

1. INTRODUCTION

The theory of stochastic integration and stochastic differential equations (SDEs), known as the Itô calculus, was first introduced by Kiyoshi Itô in 1940s. After this introduction, SDEs are preferred to be used frequently in applied mathematics due to random processes in different subjects such as physics, biology, and economics. [2, 3, 5, 10, 21, 13, 15, 20]. This paper includes stochastic biased and correlated random walk (BCRW) models in one, two, and three dimensions. Derivation steps are explained in detail only for one and two dimensions.

In nature, the direction of the movement of animals, micro-organisms, or cells is not random and usually there is a correlation between the consecutive steps of the motion. Various mathematical models incorporating the above idea of the particle motion have been developed. In Correlated Random Walk (CRW) models, the current direction of a particle is considered to be related with the previous movement direction. For instance, most animals tend to move forward. This persistence produces

a local directional bias. CRW models are commonly used to investigate the animal paths in biology or ecology [7, 12, 16, 22]. However, besides the local directional bias, some movements also have a global preferred direction towards a target such as a light or food source. These types of motion are known as a biased and correlated random walk. For example, the movement paths of swimming micro-organisms and butterflies can be modeled as BCRW [14, 19].

In this paper, stochastic partial differential equations (SPDEs) are derived for a BCRW in one, two, and three dimensions under the assumption that globally preferred direction of movement is independent of the location of the particles. Solutions of derived SPDEs, in one and two dimensions, are compared with independently formulated Monte Carlo simulations. Computational results of SPDEs are in well agreement with the results of Monte Carlo calculations. The general derivation procedure for SDEs and SPDEs are not provided in this work. The details of the derivation procedure can be found at [3, 11].

2. DERIVATION OF STOCHASTIC BCRW MODELS

In this section, SPDEs are derived for BCRW models in one, two, and three dimensions.

2.1. Derivation of Stochastic BCRW in One Dimension. In this subsection, an SPDE is derived for a one-dimensional BCRW. BCRW model can be defined as a biased telegraph equation. It is assumed that the preferred absolute direction of the movement is independent of the location, i.e., the target of the particles is assumed to be located at infinity. The derivation of biased telegraph equation is given before deriving the stochastic model.

In one dimensional case, right and left direction moving particles are considered. Notations of α and β are used to show numbers of right and left moving particles per unit distance. The rate of change for the right and left moving particles can be modeled by the following system of differential equations:

$$(2.1) \quad \frac{\partial \alpha}{\partial t} = -v \frac{\partial \alpha}{\partial x} - \gamma_1 \alpha + \gamma_2 \beta$$

$$(2.2) \quad \frac{\partial \beta}{\partial t} = v \frac{\partial \beta}{\partial x} + \gamma_1 \alpha - \gamma_2 \beta$$

where v is a constant speed, γ_1 is the rate that right-moving particles change direction to the left, and similarly, γ_2 is the rate that left-moving particles change direction to the right.

Adding equations (2.1) and (2.2) and differentiating the resulted equation with respect to t gives the following equation:

$$(2.3) \quad \frac{\partial^2(\alpha + \beta)}{\partial t^2} = v \frac{\partial^2(\beta - \alpha)}{\partial x \partial t}.$$

Subtracting the equation (2.1) from the equation (2.2) and differentiating with respect to x gives

$$(2.4) \quad \frac{\partial^2(\beta - \alpha)}{\partial x \partial t} = v \frac{\partial^2(\beta + \alpha)}{\partial x^2} - 2\gamma_2 \frac{\partial(\beta)}{\partial x} + 2\gamma_1 \frac{\partial(\alpha)}{\partial x}$$

Then, substituting the equation (2.4) into the equation (2.3), replacing $\alpha + \beta$ by p , $p = p(x, t)$ is the total particle density, and modifying the resulting equation by adding and subtracting related terms gives the biased telegraph equation:

$$(2.5) \quad \frac{\partial^2 p}{\partial t^2} + (\gamma_1 + \gamma_2) \frac{\partial p}{\partial t} + v(\gamma_2 - \gamma_1) \frac{\partial p}{\partial x} = v^2 \frac{\partial^2 p}{\partial x^2}$$

It is clear that when $\gamma_1 = \gamma_2$, assuming that turning probabilities are same, then the equation (2.5) reduces to a known telegraph equation which is used to model the CRW in one-dimension.

TABLE 1. Right-moving particle population changes on $[x_{i-1}, x_i]$ in time Δt

Possible Change ($\Delta\alpha_i$)	Probability
$\alpha_{i-1}v\Delta t/\Delta x$	$p_2 = 1$
$-\alpha_i v\Delta t/\Delta x$	$p_2 = 1$
0	$p_3 = \alpha_i \sigma v \Delta t (1 - \gamma_1)$
-1	$p_4 = \alpha_i \sigma v \Delta t \gamma_1$
1	$p_5 = \beta_i \sigma v \Delta t \gamma_2$

TABLE 2. Left-moving particle population changes on $[x_{i-1}, x_i]$ in time Δt

Possible Change ($\Delta\beta_i$)	Probability
$\beta_{i+1}v\Delta t/\Delta x$	$p_1 = 1$
$-\beta_i v\Delta t/\Delta x$	$p_2 = 1$
0	$p_3 = \beta_i \sigma v \Delta t (1 - \gamma_2)$
-1	$p_4 = \beta_i \sigma v \Delta t \gamma_2$
1	$p_5 = \alpha_i \sigma v \Delta t \gamma_1$

The derivation of a stochastic version of the biased telegraph equation in one-dimension is similar to the unbiased case which is well known as CRW, except that there are different turning probabilities depending on the direction of the movement. As summarized on page 3, in one dimensional BCRW there are right and left direction moving particles with a constant speed v . It is assumed that particles may have an interaction with probability per unit distance σ . As a result of this, a possible change in direction may occur. When a possible change in direction occurs, the probability of a right-moving particle turning left is γ_1 . Moreover, γ_2 is the probability of a left-moving particle turning right after an interaction occurs. For example, $(1 - \gamma_1)$

is the probability of a right-moving particle preserving its initial direction. Notations of $\alpha(x, t)$ and $\beta(x, t)$ are used to show the number densities of right and left moving particles at position x and time t . To find changes occurring, for a small time interval Δt , in the right and left moving particle populations, the space interval $[x_{\min}, x_{\max}]$ is divided into N sub-intervals $[x_{i-1}, x_i]$, for $i = 1, 2, \dots, N$ where $x_0 = x_{\min}$, $x_N = x_{\max}$, $x_j = x_{\min} + j\Delta x$ for $j = 1, 2, \dots, N - 1$, and $\Delta x = (x_{\max} - x_{\min})/N$. Let $\alpha_i(t)$ and $\beta_i(t)$ be numbers of right and left moving particles on the interval $[x_{i-1}, x_i]$ at time t . Possible changes for $\alpha_i(t)$ and $\beta_i(t)$ for a small time interval, Δt , are listed in Table 1 and Table 2. In Table 1, the possible changes for right moving particles on the i th interval, $[x_{i-1}, x_i]$, are listed. Because of the assumption that particles move with a constant velocity, v , right moving particles in the $(i - 1)$ st interval, $\alpha_{i-1}(t)v\frac{\Delta t}{\Delta x}$, pass into the i th interval in time period Δt with probability unity. In the same manner, right moving particles on the i th interval, $\alpha_i(t)v\frac{\Delta t}{\Delta x}$, cross into the next interval in time period Δt with probability unity. Besides, one right moving particle on the i th interval changes its direction to the left with probability $\alpha_i(t)v\sigma\gamma_1\Delta t$. Moreover, one left-moving particle changes direction and becomes a right-moving particle with probability $\beta_i(t)v\sigma\gamma_2\Delta t$. Last two terms in Table 1 build random part of the derived BCRW equation for the right moving particle population. Changes and probabilities in Table 2 are constructed for left moving particles, based on the similar argument used to form Table 1. Tables 1 and 2 define a discrete stochastic model for BCRW in one-dimension. Based on the discrete stochastic model, the particle population levels $\alpha_i(t)$ and $\beta_i(t)$ for $i = 1, 2, \dots, N$, approximately satisfy the following SDE system (2.6) and (2.7), where $\tilde{W}_i(t)$, $W_i(t)$ are independent Wiener processes for $i = 1, \dots, N$:

$$(2.6) \quad \frac{d\alpha_i(t)}{dt} = \frac{(\alpha_{i-1}(t) - \alpha_i(t))v}{\Delta x} - \alpha_i(t)\sigma v\gamma_1 + \beta_i(t)\sigma v\gamma_2 \\ - \sqrt{\alpha_i(t)\sigma v\gamma_1} \frac{d\tilde{W}_i(t)}{dt} + \sqrt{\beta_i(t)\sigma v\gamma_2} \frac{dW_i(t)}{dt}$$

$$(2.7) \quad \frac{d\beta_i(t)}{dt} = \frac{(\beta_{i+1}(t) - \beta_i(t))v}{\Delta x} - \beta_i(t)\sigma v\gamma_2 + \alpha_i(t)\sigma v\gamma_1 \\ - \sqrt{\beta_i(t)\sigma_2 v\gamma} \frac{dW_i(t)}{dt} + \sqrt{\alpha_i(t)\sigma_1 v\gamma} \frac{d\tilde{W}_i(t)}{dt}$$

In the systems (2.6) and (2.7), $\alpha_i(t)$ and $\beta_i(t)$ are replaced by $\alpha(x_i, t)\Delta x$ and $\beta(x_i, t)\Delta x$, respectively, where $\alpha(x, t)$ and $\beta(x, t)$ are the right and left moving particle population densities at position x and time t . Then, the resulting equations are divided by Δx to obtain the following system:

$$(2.8) \quad \frac{\partial\alpha(x_i, t)}{\partial t} = \frac{(\alpha(x_{i-1}, t) - \alpha(x_i, t))v}{\Delta x} - \alpha(x_i, t)\sigma v\gamma_1 + \beta(x_i, t)\sigma v\gamma_2 \\ - \sqrt{\frac{\alpha(x_i, t)\sigma v\gamma_1}{\Delta x}} \frac{d\tilde{W}_i(t)}{dt} + \sqrt{\frac{\beta(x_i, t)\sigma v\gamma_2}{\Delta x}} \frac{dW_i(t)}{dt}$$

$$(2.9) \quad \frac{\partial \beta(x_i, t)}{\partial t} = \frac{(\beta(x_{i+1}, t) - \beta(x_i, t))v}{\Delta x} - \beta(x_i, t)\sigma v\gamma_2 + \alpha(x_i, t)\sigma v\gamma_1 \\ - \sqrt{\frac{\beta(x_i, t)\sigma v\gamma_2}{\Delta x}} \frac{dW_i(t)}{dt} + \sqrt{\frac{\alpha(x_i, t)\sigma v\gamma_1}{\Delta x}} \frac{d\tilde{W}_i(t)}{dt}$$

Finally, a suitable two dimensional Brownian sheet is substituted for each Wiener process in (3.8) and (3.9), and as Δx approaches zero, the following SPDEs are derived:

$$(2.10) \quad \frac{\partial \alpha(x, t)}{\partial t} = -\frac{v\partial(\alpha(x, t))}{\partial x} - \alpha(x, t)\sigma v\gamma_1 + \beta(x, t)\sigma v\gamma_2 \\ - \sqrt{\alpha(x, t)\sigma v\gamma_1} \frac{\partial^2 \tilde{W}(t, x)}{\partial x \partial t} + \sqrt{\beta(x, t)\sigma v\gamma_2} \frac{\partial^2 W(t, x)}{\partial x \partial t}$$

$$(2.11) \quad \frac{\partial \beta(x, t)}{\partial t} = \frac{v\partial(\beta(x, t))}{\partial x} - \beta(x, t)\sigma v\gamma_2 + \alpha(x, t)\sigma v\gamma_1 \\ - \sqrt{\beta(x, t)\sigma v\gamma_2} \frac{\partial^2 W(t, x)}{\partial x \partial t} + \sqrt{\alpha(x, t)\sigma v\gamma_1} \frac{\partial^2 \tilde{W}(t, x)}{\partial x \partial t}$$

where $W(t, x)$ and $\tilde{W}(t, x)$ are two dimensional Brownian sheets. Specifically,

$$dW_i(t) = \frac{1}{\sqrt{\Delta x}} \int_{x_{i-1}}^{x_i} \frac{\partial^2 W(t, x)}{\partial x \partial t} dx dt \quad \text{for } i = 1, 2, \dots, N$$

and

$$d\tilde{W}_i(t) = \frac{1}{\sqrt{\Delta x}} \int_{x_{i-1}}^{x_i} \frac{\partial^2 \tilde{W}(t, x)}{\partial x \partial t} dx dt \quad \text{for } i = 1, 2, \dots, N.$$

2.2. Derivation of Stochastic Biased and Correlated Random Walk in Two Dimensions. Two dimensional equations are derived by considering four possible directions (right, left, up, and down) of movement providing a simpler derivation procedure than in previous work [8]. It is assumed that the preferred absolute direction of movement is independent of the location, i.e., the target of the particles is considered to be located at infinity. As in one dimensional case, particles move with a constant speed v . It is also assumed that only one event is possible in a small time interval, i.e., the interaction and movement cannot happen simultaneously at each time step Δt . Before determining the changes that occur in each rectangular region for a small interval of time, some notation is first introduced:

Let $A_1(x, y, t)$ and $A_3(x, y, t)$ be the number of right and left moving particles at position (x, y) per unit area at time t , respectively. Similarly, $A_2(x, y, t)$ and $A_4(x, y, t)$ be the number of downward and upward moving particles at position (x, y) per unit area at time t , respectively. Let σ be the probability of interaction of two particles. Let γ_1 be the probability of any particle changing its direction to the right after an interaction, γ_2 be the probability of any particle changing its direction to the downward direction, γ_3 be the probability of any particle changing its direction to

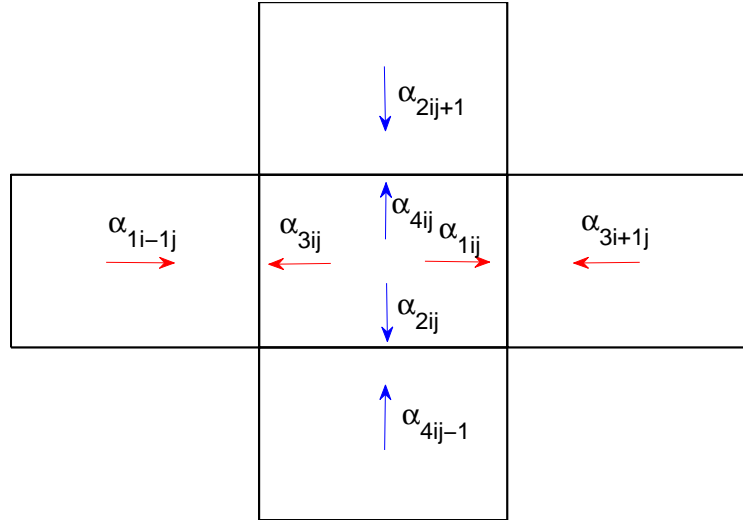


FIGURE 1. Diagram of possible changes of particles in two dimensions due to movement for $[x_i, x_{i+1}] \times [y_j, y_{j+1}]$ rectangle

the left, and γ_4 be the probability of any particle changing its direction to the upward direction. Note that $\gamma_1 + \gamma_2 + \gamma_3 + \gamma_4 = 1$.

When the change of direction probabilities are different than each other, there is a globally preferred direction for the particles. For example, if γ_1 is greater than the other turning probabilities, then the right direction is the globally preferred direction, i.e., there is a bias in the right direction. In time, the number of right moving particles will increase.

First, a discrete stochastic model is derived. To do this, the plane is made discrete by dividing $[x_{\min}, x_{\max}] \times [y_{\min}, y_{\max}]$ into I and J equal intervals, respectively. Let $\Delta x = x_{i+1} - x_i$, for $i = 0, 1, 2 \dots I - 1$, and $\Delta y = y_{j+1} - y_j$, for $j = 0, 1, 2 \dots J - 1$. So, the summation $\sum_{k=1}^4 \int_{x_i}^{x_{i+1}} \int_{y_j}^{y_{j+1}} A_k(x, y, t) dy dx$ gives the total number of particles on the rectangle $[x_i, x_{i+1}] \times [y_j, y_{j+1}]$. Define $\alpha_{kij} = A_k(x_i, y_j, t) \Delta x \Delta y$ for $k = 1, 2, 3, 4$. Thus, for example, α_{1ij} is the total number of particles moving in the right direction in region $[x_i, x_{i+1}] \times [y_j, y_{j+1}]$ at time t . The other directions are defined similarly.

Diagram of possible changes of particles in two dimensions due to movement for $[x_i, x_{i+1}] \times [y_j, y_{j+1}]$ rectangle is given in Figure 1. In addition, a possible change of particles before and after an interaction in two dimensions for $[x_i, x_{i+1}] \times [y_j, y_{j+1}]$ rectangle is represented in Figure 2. Table 3 defines a discrete stochastic model for α_{1ij} . The changes and the probabilities are shown. For instance, $\alpha_{1i-1j} v \Delta t / \Delta x$ particles go from $[x_{i-1}, x_i] \times [y_j, y_{j+1}]$ into $[x_i, x_{i+1}] \times [y_j, y_{j+1}]$ with probability 1. In addition, particles are coming in or going out of $[x_i, x_{i+1}] \times [y_j, y_{j+1}]$ in the right

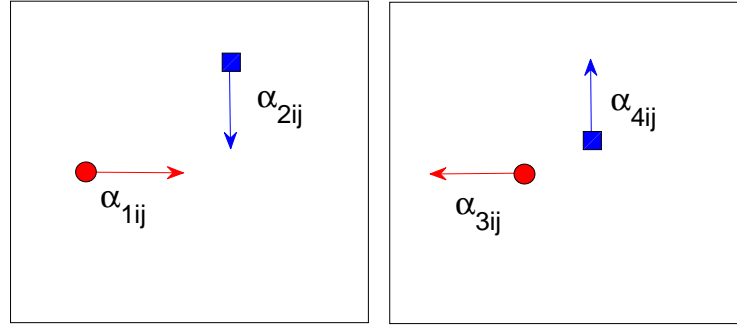


FIGURE 2. Representation of a possible change of particles before and after an interaction in two dimensions for $[x_i, x_{i+1}] \times [y_j, y_{j+1}]$ rectangle

TABLE 3. Changes and probabilities for the number of particles moving in right direction in rectangle $[x_i, x_{i+1}] \times [y_j, y_{j+1}]$ for two-dimensional BCRW

Possible Change ($\Delta\alpha_{1ij}$)	Probability
$\alpha_{1i-1j}v\Delta t/\Delta x$	1
$-\alpha_{1ij}v\Delta t/\Delta x$	1
+1	$\alpha_{2ij}\sigma v\lambda_1\Delta t$
+1	$\alpha_{3ij}\sigma v\lambda_1\Delta t$
+1	$\alpha_{4ij}\sigma v\lambda_1\Delta t$
0	$\alpha_{1ij}\sigma v(1 - \lambda_2 - \lambda_3 - \lambda_4)\Delta t$
-1	$\alpha_{1ij}\sigma v\lambda_4\Delta t$
-1	$\alpha_{1ij}\sigma v\lambda_2\Delta t$
-1	$\alpha_{1ij}\sigma v\lambda_3\Delta t$

direction. The third line in Table 3 is an addition of one right moving particle due to interaction and direction change of a particle moving in the downward direction. The fourth and fifth lines of the table are defined similarly. The last three lines represent the loss of a right moving particle due to direction change as a result of an interaction.

The stochastic models in Tables 4, 5 and 6 are created similarly as those in Table 3. Based on the changes and probabilities in Tables 3, 4, 5, and 6, the particle population levels α_i for $i = 1, 2, 3, 4$ approximately satisfy the following SDE system:

$$\begin{aligned}
 (2.12) \quad \frac{d\alpha_{1ij}(t)}{dt} = & \frac{(\alpha_{1i-1j}(t) - \alpha_{1ij}(t))v}{\Delta x} + \sum_{k=2}^4 \alpha_{kij}\sigma v\lambda_1 - \sum_{k=2}^4 \alpha_{1ij}\sigma v\lambda_k \\
 & + \sum_{k=2}^4 \sqrt{\alpha_{kij}\sigma v\lambda_1} \frac{dW_{k1ij}(t)}{dt} - \sum_{k=2}^4 \sqrt{\alpha_{1ij}\sigma v\lambda_k} \frac{dW_{1kij}(t)}{dt}
 \end{aligned}$$

TABLE 4. Changes and probabilities for the number of particles moving in downward direction in rectangle $[x_i, x_{i+1}] \times [y_j, y_{j+1}]$ for two-dimensional BCRW

Possible Change ($\Delta\alpha_{2ij}$)	Probability
$\alpha_{2ij+1}v\Delta t/\Delta y$	1
$-\alpha_{2ij}v\Delta t/\Delta y$	1
+1	$\alpha_{1ij}\sigma v\lambda_2\Delta t$
+1	$\alpha_{3ij}\sigma v\lambda_2\Delta t$
+1	$\alpha_{4ij}\sigma v\lambda_2\Delta t$
0	$\alpha_{2ij}\sigma v(1 - \lambda_1 - \lambda_3 - \lambda_4)\Delta t$
-1	$\alpha_{2ij}\sigma v\lambda_1\Delta t$
-1	$\alpha_{2ij}\sigma v\lambda_4\Delta t$
-1	$\alpha_{2ij}\sigma v\lambda_3\Delta t$

TABLE 5. Changes and probabilities for the number of particles moving in left direction in rectangle $[x_i, x_{i+1}] \times [y_j, y_{j+1}]$ for two-dimensional BCRW

Possible Change ($\Delta\alpha_{3ij}$)	Probability
$\alpha_{3i+1j}v\Delta t/\Delta x$	1
$-\alpha_{3ij}v\Delta t/\Delta x$	1
+1	$\alpha_{4ij}\sigma v\lambda_3\Delta t$
+1	$\alpha_{1ij}\sigma v\lambda_3\Delta t$
+1	$\alpha_{2ij}\sigma v\lambda_3\Delta t$
0	$\alpha_{3ij}\sigma v(1 - \lambda_1 - \lambda_2 - \lambda_4)\Delta t$
-1	$\alpha_{3ij}\sigma v\lambda_1\Delta t$
-1	$\alpha_{3ij}\sigma v\lambda_2\Delta t$
-1	$\alpha_{3ij}\sigma v\lambda_4\Delta t$

$$\begin{aligned}
 (2.13) \quad \frac{d\alpha_{2ij}(t)}{dt} &= \frac{(\alpha_{2ij+1}(t) - \alpha_{2ij}(t))v}{\Delta y} + \sum_{\substack{k=1 \\ k \neq 2}}^4 \alpha_{kij}\sigma v\lambda_2 - \sum_{\substack{k=1 \\ k \neq 2}}^4 \alpha_{2ij}\sigma v\lambda_k \\
 &+ \sum_{\substack{k=1 \\ k \neq 2}}^4 \sqrt{\alpha_{kij}\sigma v\lambda_2} \frac{dW_{k2ij}(t)}{dt} - \sum_{\substack{k=1 \\ k \neq 2}}^4 \sqrt{\alpha_{2ij}\sigma v\lambda_k} \frac{dW_{2kij}(t)}{dt}
 \end{aligned}$$

TABLE 6. Changes and probabilities for the number of particles moving in upward direction in rectangle $[x_i, x_{i+1}] \times [y_j, y_{j+1}]$ for two-dimensional BCRW

Possible Change ($\Delta\alpha_{4ij}$)	Probability
$\alpha_{4ij-1}v\Delta t/\Delta y$	1
$-\alpha_{4ij}v\Delta t/\Delta y$	1
+1	$\alpha_{1ij}\sigma v\lambda_4\Delta t$
+1	$\alpha_{2ij}\sigma v\lambda_4\Delta t$
+1	$\alpha_{3ij}\sigma v\lambda_4\Delta t$
0	$\alpha_{4ij}\sigma v(1 - \lambda_1 - \lambda_2 - \lambda_3)\Delta t$
-1	$\alpha_{4ij}\sigma v\lambda_1\Delta t$
-1	$\alpha_{4ij}\sigma v\lambda_2\Delta t$
-1	$\alpha_{4ij}\sigma v\lambda_3\Delta t$

$$\begin{aligned}
 (2.14) \quad \frac{d\alpha_{3ij}(t)}{dt} &= \frac{(\alpha_{3i+1j}(t) - \alpha_{3ij}(t))v}{\Delta x} + \sum_{\substack{k=1 \\ k \neq 3}}^4 \alpha_{kij}\sigma v\lambda_3 - \sum_{\substack{k=1 \\ k \neq 3}}^4 \alpha_{3ij}\sigma v\lambda_k \\
 &+ \sum_{\substack{k=1 \\ k \neq 3}}^4 \sqrt{\alpha_{kij}\sigma v\lambda_3} \frac{dW_{k3ij}(t)}{dt} - \sum_{\substack{k=1 \\ k \neq 3}}^4 \sqrt{\alpha_{3ij}\sigma v\lambda_k} \frac{dW_{3kij}(t)}{dt}
 \end{aligned}$$

$$\begin{aligned}
 (2.15) \quad \frac{d\alpha_{4ij}(t)}{dt} &= \frac{(\alpha_{4ij-1}(t) - \alpha_{4ij}(t))v}{\Delta y} + \sum_{k=1}^3 \alpha_{kij}\sigma v\lambda_4 - \sum_{k=1}^3 \alpha_{4ij}\sigma v\lambda_k \\
 &+ \sum_{k=1}^3 \sqrt{\alpha_{kij}\sigma v\lambda_4} \frac{dW_{k4ij}(t)}{dt} - \sum_{k=1}^3 \sqrt{\alpha_{4ij}\sigma v\lambda_k} \frac{dW_{4kij}(t)}{dt}
 \end{aligned}$$

Moreover, an SPDE system is derived for this problem. First, the equations (2.12)-(2.15), are all divided by $\Delta x \Delta y$. Then, $\alpha_{kij}/\Delta x \Delta y$ is changed by $A_k(x_i, y_j, t)$ for $k = 1, 2, 3, 4$. Next, a suitable three dimensional Brownian sheet is substituted for each Wiener process in (2.12)-(2.15). As Δx and Δy approach 0, SPDE system

is derived:

$$\begin{aligned}
 (2.16) \quad \frac{\partial A_1(x, y, t)}{\partial t} &= -v \frac{\partial A_1(x, y, t)}{\partial x} + \sum_{k=2}^4 A_k(x, y, t) \sigma v \lambda_1 \\
 &\quad - \sum_{k=2}^4 A_1(x, y, t) \sigma v \lambda_k \\
 &\quad + \sum_{k=2}^4 \sqrt{A_k(x, y, t)} \sigma v \lambda_1 \frac{\partial^3 W_{k1}(x, y, t)}{\partial x \partial y \partial t} \\
 &\quad + \sum_{k=2}^4 -\sqrt{A_1(x, y, t)} \sigma v \lambda_k \frac{\partial^3 W_{1k}(x, y, t)}{\partial x \partial y \partial t}
 \end{aligned}$$

$$\begin{aligned}
 (2.17) \quad \frac{\partial A_2(x, y, t)}{\partial t} &= v \frac{\partial A_2(x, y, t)}{\partial y} + \sum_{\substack{k=1 \\ k \neq 2}}^4 A_k(x, y, t) \sigma v \lambda_2 \\
 &\quad - \sum_{\substack{k=1 \\ k \neq 2}}^4 A_2(x, y, t) \sigma v \lambda_k \\
 &\quad + \sum_{\substack{k=1 \\ k \neq 2}}^4 \sqrt{A_k(x, y, t)} \sigma v \lambda_2 \frac{\partial^3 W_{k2}(x, y, t)}{\partial x \partial y \partial t} \\
 &\quad - \sum_{\substack{k=1 \\ k \neq 2}}^4 \sqrt{A_2(x, y, t)} \sigma v \lambda_k \frac{\partial^3 W_{2k}(x, y, t)}{\partial x \partial y \partial t}
 \end{aligned}$$

$$\begin{aligned}
 (2.18) \quad \frac{\partial A_3(x, y, t)}{\partial t} &= v \frac{\partial A_3(x, y, t)}{\partial x} + \sum_{\substack{k=1 \\ k \neq 3}}^4 A_k(x, y, t) \sigma v \lambda_3 \\
 &\quad - \sum_{\substack{k=1 \\ k \neq 3}}^4 A_3(x, y, t) \sigma v \lambda_k \\
 &\quad + \sum_{\substack{k=1 \\ k \neq 3}}^4 \sqrt{A_k(x, y, t)} \sigma v \lambda_3 \frac{\partial^3 W_{k3}(x, y, t)}{\partial x \partial y \partial t} \\
 &\quad - \sum_{\substack{k=1 \\ k \neq 3}}^4 \sqrt{A_3(x, y, t)} \sigma v \lambda_k \frac{\partial^3 W_{3k}(x, y, t)}{\partial x \partial y \partial t}
 \end{aligned}$$

$$\begin{aligned}
(2.19) \quad \frac{\partial A_4(x, y, t)}{\partial t} &= -v \frac{\partial A_4(x, y, t)}{\partial y} + \sum_{k=1}^3 A_k(x, y, t) \sigma v \lambda_4 \\
&\quad - \sum_{k=1}^3 A_4(x, y, t) \sigma v \lambda_k \\
&\quad + \sum_{k=1}^3 \sqrt{A_k(x, y, t) \sigma v \lambda_4} \frac{\partial^3 W_{k4}(x, y, t)}{\partial x \partial y \partial t} \\
&\quad - \sum_{k=1}^3 \sqrt{A_4(x, y, t) \sigma v \lambda_k} \frac{\partial^3 W_{4k}(x, y, t)}{\partial x \partial y \partial t}
\end{aligned}$$

where, for example,

$$dW_{21ij}(t) = \frac{1}{\sqrt{\Delta x \Delta y}} \int_{y_j}^{y_{j+1}} \int_{x_i}^{x_{i+1}} \frac{\partial^3 W_{21}(x, y, t)}{\partial x \partial y \partial t} dx dy dt$$

This model reduces to unbiased correlated random walk model if $\lambda_1 = \lambda_2 = \lambda_3 = \lambda_4$.

2.3. SPDE for BCRW in Three Dimensions. In an analogous way, it is straightforward to derive the stochastic partial differential equations for BCRW in three dimensions. It is assumed that there are only six possible movement directions. The resulting SPDE for right moving particles has the following form:

$$\begin{aligned}
(2.20) \quad \frac{\partial A_1(x, y, z, t)}{\partial t} &= -v \frac{\partial A_1(x, y, z, t)}{\partial x} \\
&\quad + \sum_{k=2}^6 A_k(x, y, z, t) \sigma v \lambda_1 - \sum_{k=2}^6 A_1(x, y, z, t) \sigma v \lambda_k \\
&\quad + \sum_{k=2}^6 \sqrt{A_k(x, y, z, t) \sigma v \lambda_1} \frac{\partial^4 W_{k1}(x, y, z, t)}{\partial x \partial y \partial z \partial t} \\
&\quad - \sum_{k=2}^6 \sqrt{A_1(x, y, z, t) \sigma v \lambda_k} \frac{\partial^4 W_{1k}(x, y, z, t)}{\partial x \partial y \partial z \partial t}
\end{aligned}$$

The equations for the particles moving in different directions can be derived in a similar manner.

3. COMPARISON OF NUMERICAL SOLUTIONS

In this part, one and two dimensional derived SPDEs for BCRW are solved numerically by Euler's Maruyama method and results are compared with the independently formulated Monte Carlo (MC) calculations [18, 17]. An identical initial distribution is considered for each computer experiment.

In the first part, derived one dimensional stochastic partial differential equations, (2.10) and (2.11), are numerically solved. Specifically, an Euler- Maruyama approximation to this SDE system, including (2.6) and (2.7), is used and given by:

$$(3.1) \quad \alpha_i(t + \Delta t) \approx \alpha_i(t) + \alpha_{i-1}(t)v\Delta t/\Delta x - \alpha_i(t)v\Delta t/\Delta x - \alpha_i(t)\sigma v\Delta t\gamma_1 \\ + \beta_i(t)\sigma v\Delta t\gamma_2 - \sqrt{\alpha_i(t)\sigma v\Delta t\gamma_1}\tilde{\nu}_i + \sqrt{\beta_i(t)\sigma v\Delta t\gamma_2}\nu_i$$

$$(3.2) \quad \beta_i(t + \Delta t) \approx \beta_i(t) + \beta_{i+1}(t)v\Delta t/\Delta x - \beta_i(t)v\Delta t/\Delta x - \beta_i(t)\sigma v\Delta t\gamma_2 \\ + \alpha_i(t)\sigma v\Delta t\gamma_1 - \sqrt{\beta_i(t)\sigma v\Delta t\gamma_2}\nu_i + \sqrt{\alpha_i(t)\sigma v\Delta t\gamma_1}\tilde{\nu}_i$$

where $\nu_i, \tilde{\nu}_i$, are independent normally distributed numbers with mean zero and variance unity for $i = 1, \dots, N$.

According to the initial distribution, there are 2800 particles on the interval $[-5, 5]$. The distribution of right and left moving particles are assumed to be identical. The Number of the right and left moving particles are 150 on $[-5, -2] \cup [2, 5]$, $325x + 800$ on $(-2, 0]$, and $800 - 325x$ on $[0, 2)$. Particles move continuously with a constant velocity $v = 1$. Particles get an interaction with probability per unit distance $\sigma = 1$. After an interaction occurs, the probability for right moving particles changing direction is 0.1 and similarly the probability for left moving particles changing direction is 0.9. Distribution of the total number of particles on the interval $[-1.25, 1.25]$ is observed at time 0.5.

In the numerical solution of the SPDEs, Δx and Δt are selected sufficiently small to obtain an accurate approximation. For example, the position interval $[-5, 5]$ is divided into 1280 sub-intervals and time is divided into 200 sub-intervals such that $\Delta t = \frac{\text{total time}}{200}$. In the MC simulation, particles are tracked individually to check for an interaction or direction change at each time step. For both of those independently formulated programs, 500 sample paths are used to get accurate statistical results. In Table 7, mean numbers and standard deviations of the right-moving particles on $[-1.25, 1.25]$ are calculated at times 0.0625, 0.125, 0.25, 0.5 by the numerical solution of the SPDE and the MC simulation. Similar results are given for left-moving particles in Table 8. Because of the global directional bias to the right, the number of right-moving particles increases due to the scattering of left-moving particles. However at further times the value of the right moving particles are observed to decrease as well since once particles leave the spatial interval $[-5, 5]$ they do not come back. In Figure 3 mean numbers of right and left moving particles are given separately for both SPDE and MC calculations at time 0.5 on the interval $[-1.25, 1.25]$. Similarly standard deviations in the right and left moving particles are given in Figure 4 on $[-1.25, 1.25]$ at time 0.5 for both computational approaches. Tables and figures prove that two different computational procedures provide similar results.

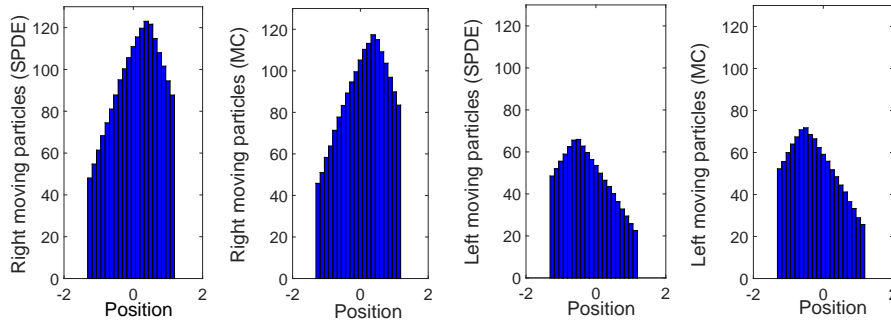


FIGURE 3. Mean number of particles on $[-1.25, 1.25]$ at time 0.5 for SPDE and MC

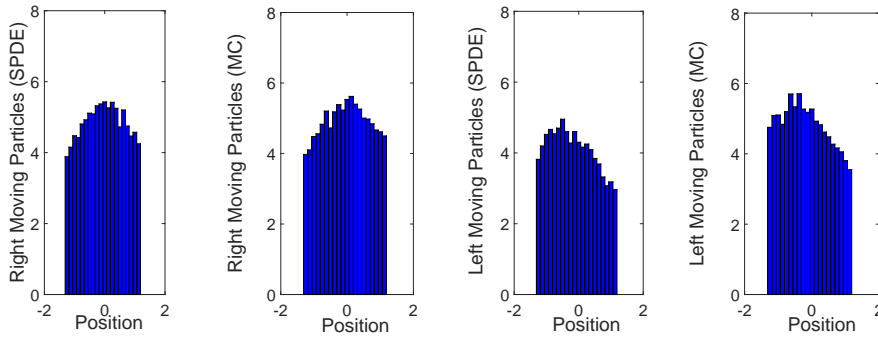


FIGURE 4. Standard deviations in the particles on $[-1.25, 1.25]$ at time 0.5 for SPDE and MC

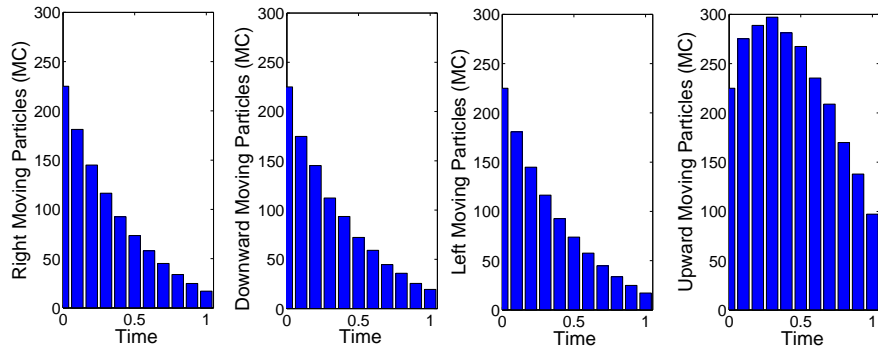
TABLE 7. Mean numbers and standard deviations (SD) of right moving particles by one-dimensional Monte Carlo (MC) and SPDE calculational results for 500 sample paths

Time	Mean of $\alpha(\text{SDE})$	Mean of $\alpha(\text{MC})$	SD of $\alpha(\text{SDE})$	SD of $\alpha(\text{MC})$
.0625	1991.3862	1988.0055	10.6121	10.5712
.125	2077.7744	2064.7517	14.2127	13.9821
.25	2226.2217	2189.0879	19.1703	18.8414
.5	2453.0867	2332.2134	23.5584	21.8746

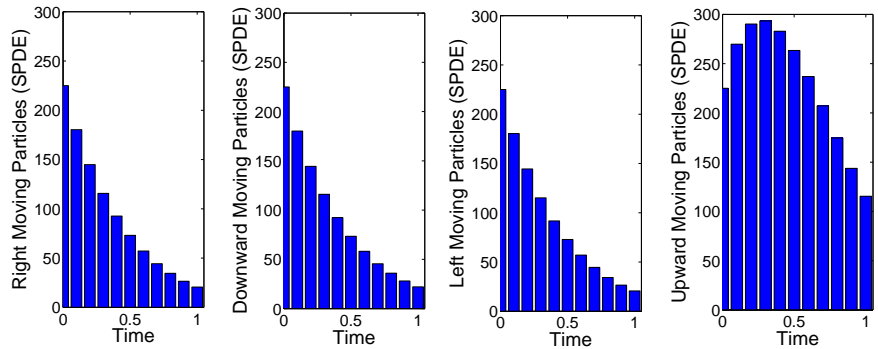
In the second part, numerical solutions of two-dimensional SPDE equations are compared with Monte Carlo calculations for two different turning probabilities. It is assumed that the velocity of the particles is constant, $v = 1$ and there are 225 right, downward, left, and upward moving particles for a total of 900 particles. Particles are uniformly distributed on $[0, 1] \times [0, 1]$. Initially, there are no particles outside of the square. The distribution of the particles on $[0, 1] \times [0, 1]$ is watched until time

TABLE 8. Mean numbers and standard deviations (SD) of left moving particles by one dimensional Monte Carlo (MC) and SPDE calculational results for 500 sample paths

Time	Mean of $\beta(\text{SDE})$	Mean of $\beta(\text{MC})$	SD of $\beta(\text{SDE})$	SD of $\beta(\text{MC})$
.0625	1807.2618	1809.9921	10.7935	10.5119
.125	1717.2837	1729.2633	13.9732	13.9642
.25	1554.5504	1592.5887	18.9341	18.8944
.5	1273.8884	1398.9347	22.7239	22.0114



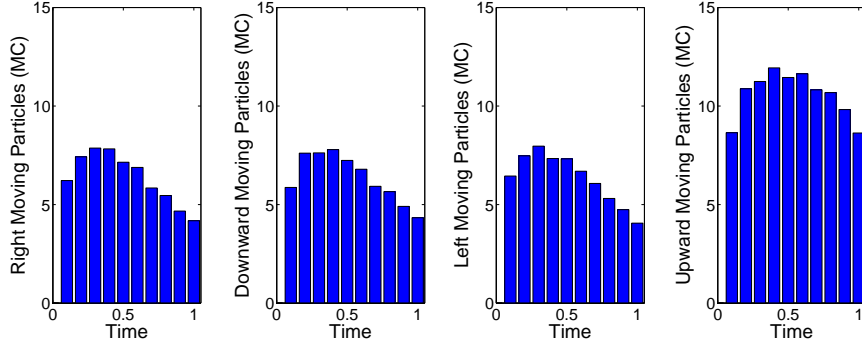
(A) Monte Carlo



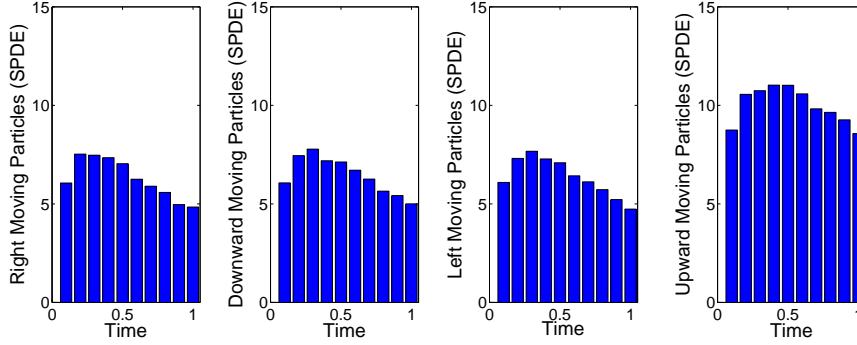
(B) SPDE

FIGURE 5. Mean number of particles in $[0, 1] \times [0, 1]$ from time 0 to time 1 for $\lambda_1 = 0.1$, $\lambda_2 = 0.1$, $\lambda_3 = 0.1$, and $\lambda_4 = 0.7$

= 1.0. The unit square is divided into 256 smaller squares. To study this problem computationally, (2.12)-(2.15) are solved numerically. For this, an Euler-Maruyama



(A) Monte Carlo



(B) SPDE

FIGURE 6. Standard deviation in number of particles in $[0, 1] \times [0, 1]$ from time 0 to time 1 for $\lambda_1 = 0.1$, $\lambda_2 = 0.1$, $\lambda_3 = 0.1$, and $\lambda_4 = 0.7$

approximation to the equation (2.12) is used:

$$\begin{aligned}
 (3.3) \quad \alpha_{1ij}(t + \Delta t) - \alpha_{1ij}(t) &\approx \frac{(\alpha_{1i-1j}(t) - \alpha_{1ij}(t))v\Delta t}{\Delta x} \\
 &+ \alpha_{2ij}\sigma v\lambda_1\Delta t + \alpha_{3ij}\sigma v\lambda_1\Delta t + \alpha_{4ij}\sigma v\lambda_1\Delta t \\
 &- \alpha_{1ij}\sigma v\lambda_4\Delta t - \alpha_{1ij}\sigma v\lambda_2\Delta t - \alpha_{1ij}\sigma v\lambda_3\Delta t \\
 &+ \sqrt{\alpha_{2ij}\sigma v\lambda_1}\eta_{21ij} + \sqrt{\alpha_{3ij}\sigma v\lambda_1}\eta_{31ij} \\
 &+ \sqrt{\alpha_{4ij}\sigma v\lambda_1}\eta_{41ij} - \sqrt{\alpha_{1ij}\sigma v\lambda_4}\eta_{14ij} \\
 &- \sqrt{\alpha_{1ij}\sigma v\lambda_2}\eta_{12ij} - \sqrt{\alpha_{1ij}\sigma v\lambda_3}\eta_{13ij}
 \end{aligned}$$

where $\alpha_{1ij}(t)$ is the number of right moving particles at time t . Besides, η_{k1ij} and η_{l1ij} for $i = 0, 1, 2, \dots, 15$, $j = 0, 1, 2, \dots, 15$, $k = 2, 3, 4$, and $l = 2, 3, 4$ are normally distributed numbers with mean 0 and variance 1. Similar approximations are used for equations (2.13)-(2.15). In the Monte Carlo simulation, each particle is tracked individually and checked for a direction change at each time step.

In the first case considered, the turning probabilities are $\lambda_1 = 0.1$, $\lambda_2 = 0.1$, $\lambda_3 = 0.1$, and $\lambda_4 = 0.7$. That is, there is a global bias in the upward direction

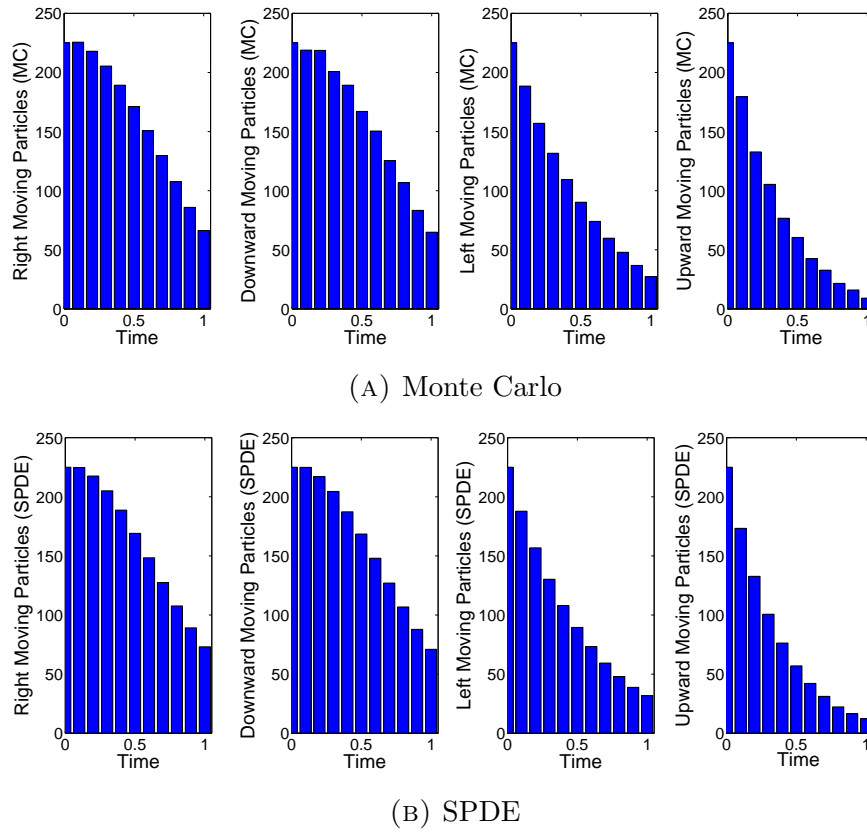


FIGURE 7. Mean number of particles in $[0, 1] \times [0, 1]$ from time 0 to time 1 for $\lambda_1 = 0.4$, $\lambda_2 = 0.4$, $\lambda_3 = 0.15$, and $\lambda_4 = 0.05$

whereas the turning probabilities are smaller for the other directions. The means and standard deviations of the number of particles in unit square at time 1 are given for 1000 sample paths. In Figure 5, the means of SPDE and MC calculations are also graphed for the same case with 1000 sample paths. Besides, the standard deviations are graphed in Figure 6 for two methods. Tables and graphs show that two approaches are in good agreement for the first case.

In the second case, turning probabilities are assumed to be $\lambda_1 = 0.4$, $\lambda_2 = 0.4$, $\lambda_3 = 0.15$, and $\lambda_4 = 0.05$. That is, there is an equal global bias in the right and downward directions. The turning probabilities for left and upward directions are smaller. In Figures 7 and 8, the means and standard deviations are given from time 0 up to time 1. SPDE and MC also are in good agreement in the second case.

4. SUMMARY AND CONCLUSIONS

We have demonstrated that the method of derivation of the stochastic correlated random walk models given by Bulut (2012) can be extended to a biased correlated random walk, where globally preferred direction is considered besides the local directional bias. In this paper, stochastic partial differential equations are derived for

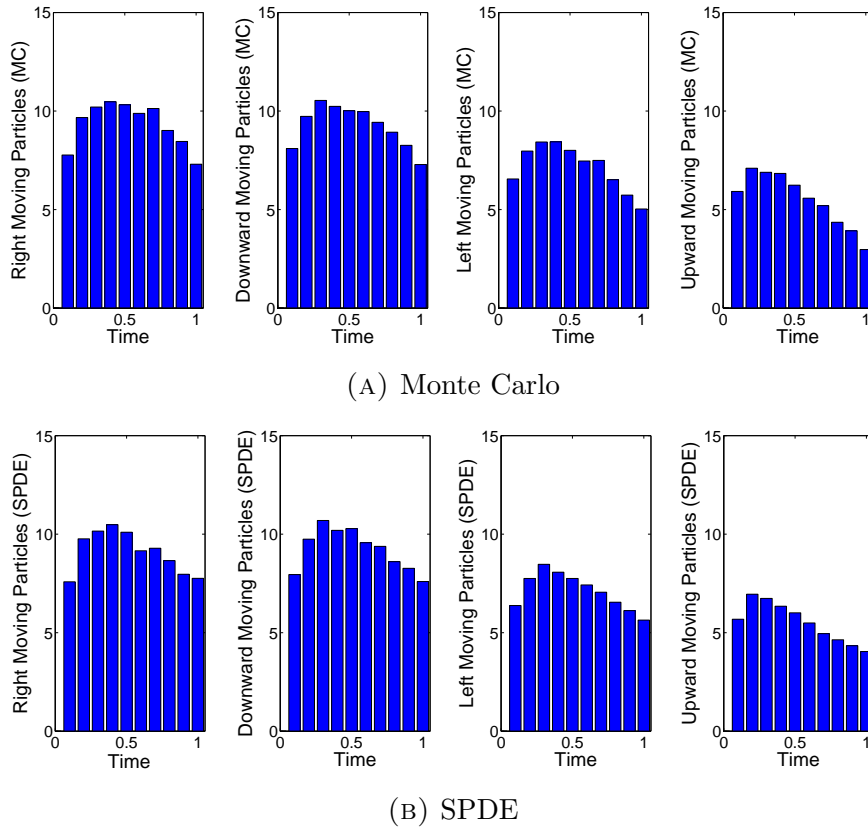


FIGURE 8. Standard deviation in number of particles in $[0, 1] \times [0, 1]$ from time 0 to time 1 for $\lambda_1 = 0.4$, $\lambda_2 = 0.4$, $\lambda_3 = 0.15$, and $\lambda_4 = 0.05$

biased and correlated random walk models in one, two, and three dimensions. In one and two dimensional cases, numerical results of derived SPDEs are compared with Monte Carlo calculations. A good agreement between two independently formulated numerical procedures supports the validity of the derived SPDEs.

The initial assumptions for the models in this article may not be relevant to every random walk models in the literature. For instance, we assumed that all particles move with a constant velocity. However, this may not represent the case when the particles have varying velocities depending on the environmental factors and changes. Besides that, the target might be located at a position different than infinity. In this case, the preferred direction depends on the location of the particles and should be carefully considered.

ACKNOWLEDGEMENT

We acknowledge the suggestions and computational assistance of Professor Edward J. Allen.

REFERENCES

- [1] E. J. Allen, Derivation of stochastic partial differential equations, *Stoch. Anal. Appl.*, 26: 357–378, 2008.
- [2] E. J. Allen, Derivation of stochastic partial differential equations for size- and age-structured populations, *J. Biol. Dyn.*, 3: 73–86, 2009.
- [3] E. J. Allen, *Modeling with Itô stochastic differential equations*, Springer, Dordrecht, 2007.
- [4] E. J. Allen, L. J. S. Allen, A. Arciniega, and P. E. Greenwood, Construction of equivalent stochastic differential equation models, *Stoch. Anal. Appl.*, 26: 274–297, 2008.
- [5] L. J. S. Allen, *An Introduction to Stochastic Processes with Applications to Biology*, Pearson Education Inc., Upper Saddle River, New Jersey, 2010.
- [6] E. J. Allen, S. J. Novosel, and Z. Zhang Finite element and difference approximation of some linear stochastic partial differential equations, *Stoch. Stoch. Rep.*, 64: 117–142, 1998.
- [7] P. Bovet and S. Benhamou, Spatial analysis of animals movements using a correlated random walk model, *J. Theor. Biol.*, 131: 419–433, 1988.
- [8] U. Bulut and E. J. Allen, Derivation of SPDEs for correlated random walk transport models in one and two dimensions, *Stoch. Anal. Appl.*, 30: 553–567, 2012.
- [9] E. M. Appell, The vibrating string forced by white noise, *Z. Wahrscheinlichkeit.*, 15: 111–130, 1970.
- [10] V. Capasso and D. Bakstein, *An Introduction to Continuous-Time Stochastic Processes*, Birkhäuser, Boston, 2012.
- [11] E. Dogan, E. J. Allen, Derivation of stochastic partial differential equations for reaction-diffusion processes, *Stoch. Anal. Appl.*, 29: 424–443, 2011.
- [12] E. A. Codling, M. J. Plank and S. Benhamou, Random walk models in biology, *J. R. Soc. Interface*, 5: 813–834, 2008.
- [13] T. C. Gard, *Introduction to Stochastic Differential Equations*, Marcel Decker, New York, 1988.
- [14] N. A. Hill, D. P. Hader, A biased random walk model for the trajectories of swimming micro-organisms, *J. Theor. Biol.*, 3186: 503–526, 1997.
- [15] H. Holden and B. Øksendal, and T. Zhang, *Stochastic Partial Differential Equations: A Modeling, White Noise Functional Approach*, Birkhäuser, Boston, Massachusetts, 1996.
- [16] P. M. Kareiva and N. Shigesada, Analyzing insect movement as a correlated random walk, *Oecologia*, 56: 234–238, 1983.
- [17] P. E. Kloeden and E. Platen, *Numerical Solution of Stochastic Differential Equations*, Springer Verlag, New York, 1992.
- [18] P. E. Kloeden, E. Platen and H. Schurz, *Numerical Solution of SDE Through Computer Experiments*, Springer, Berlin, 2003.
- [19] E. J. B. McIntire, G. Rompre and P.M. Severns, Biased correlated random walk and foray loop: which movement hypothesis drives a butterfly metapopulation?, *Oecologia*, 172: 293–305, 2012.
- [20] E. Pardoux and A. Rascanu, *Stochastic Differential Equations, Backward SDEs, Partial Differential Equations*, Springer International Publishing, Switzerland, 2014.
- [21] G. Da Prato and L. Tubaro, *Stochastic Partial Differential Equations and Applications VII*, CRC Press, Taylor & Francis Group, Boca Raton, Florida, 2006.
- [22] D. P. Siniff, C. R. Jessen and P. Zabreiko, A simulation model of animal movement patterns, *Dv. Ecol. Res.*, 6: 185–219, 1969.
- [23] J. B. Walsh, An introduction to stochastic partial differential equations, *Lect. Notes Math.*, 1180: 265–439, 1986.